

DESIGN AND EXPERIMENTAL VALIDATION OF HYDRAULIC YAW SYSTEM FOR MULTI MW WIND TURBINE

Soeren Stubkier¹, Henrik C. Pedersen² and Torben O. Andersen²

¹Hydratech Industries, Wind Power, Suensonsvej 14, 8600 Silkeborg, Denmark

²Aalborg University, Energy Technology, Pontoppidanstræde 101, 9220 Aalborg, Denmark
sst@hydratech-industries.com, hcp@et.aau.dk, toa@et.aau.dk

Abstract

To comply with the increasing demands for life time and reliability of wind turbines as these grow in size, new measures needs to be taken in the design of wind turbines and components hereof. One critical point is the initial testing of the components and systems before they are implemented in an actual turbine. Full scale hardware testing is both extremely expensive and time consuming, and so the wind turbine industry moves more towards simulations when testing.

In order to meet these demands it is necessary to use valid system models of in order to introduce new technologies to the wind turbine market. A hydraulic yaw system is such a new technology, and so a mathematical model of the full scale system and test rig system is derived and compared to measurements from the system. This is done in order to have a validated model, which wind turbine manufacturers may use for test in their simulation environment. The model and the test rig are tested against different design load cases and the results are compared. The experiments show that the model is valid for comparing the overall dynamics of the hydraulic yaw system. Based on the results it is concluded that the model derived is suitable for testing of the dynamic behavior in wind turbine manufacturer's full scale aero elastic code.

Keywords: hydraulic, yaw, model, test rig, verification

1 Introduction

For many years wind turbines have been growing in size and turbines are now being developed in the range of 5 - 10 MW. The physical sizes of these turbines are in the order of 180 - 200 meters in full height and rotor diameters of 160 - 170 meters. These extreme sizes along with the stochastic nature of the wind leads to very high demands for the wind turbine structure, sub-systems and components. Further, the expected life time for a wind turbine is now stretching from 20 to 25 years with an availability expectancy of 95 % for the entire turbine.

The yaw system of a wind turbine is a critical system which makes sure the wind turbine rotor plane always is perpendicular to the wind direction. It is important to keep the rotor plane facing the wind direction as closely as possible. Below rated wind speed¹ a yaw error would mean lower power output and above rated wind speed the loading of the wind turbine and components hereof is increased when there is a yaw error.

Yaw systems have had many designs through the history of wind turbines. They have been controlled by

a large wind vane placed behind the rotor plane, a small wind wheel as known from the old fashioned Dutch wind mills, all the way to today's most widely used yaw system with electrical gear motors. Figure 1 illustrates a wind turbine nacelle including an indication of the yaw system.



Fig. 1: Illustration of wind turbine nacelle incl. yaw system

This manuscript was received on 21 December 2012 and was accepted after revision for publication on 29 April 2013

¹Rated wind speed is the wind speed, where the turbine is producing its maximum power output and the pitch system of the turbine starts turning the blades out of the wind to control the power input to the generator.

Today normal yaw systems consist of a number of small electrical motors each in the 2 - 3 kW range and typically mounted with a planetary gear with a reduction of 1:1000. There is a further gear reduction from pinion to tooth-rim of 15 - 20. The number of drives range between two and 16 depending on the size of the turbine and design of the yaw system.

The nacelle is placed on either a roller/ball bearing or a friction plate bearing. If the low friction roller/ball bearing solution is chosen it is in combination with a huge disc brake with the same diameter as the tooth-rim and multiple brake calibers. When this system yaws, the brakes are released and the electrical motors turn until the rotor plane is in the right place, where the motors are stopped and the brakes once again engaged. For the system with friction bearing the motors are simply turned on adding enough torque to overcome the friction, hence yawing the system. It should be noticed that these simple movements are done with loadings of up to 25 MNm at a frequency of approx. 0.5 Hz.

The wind direction is normally determined by a wind vane placed on the back of the nacelle, behind the rotor plane of the turbine, which gives very noisy and inaccurate measurements; hence the direction measurement is based on average values with large hysteresis on the movement.

The electrical motors in combination with the gear, pinion and tooth-rim has been the wind turbine manufactures preferred yaw system solution for the last 20 years or so. However, as the turbines grow in size new measures needs to be taken. One very practical problem is simply space for the drives in the nacelle. Also the poor wind direction measurement and the fact that the number of activations are kept at a minimum, to reduce loading, results in lower annual power production. The latter may be seen in that an average yaw error for a wind turbine is between 5 - 10 degrees, yielding a reduced power output of approx. 2 % annually (Pedersen, 2011).

On the mechanical side problems occur when up to 16 drives in connection with huge gear reductions are started at once. Some of the drives might be in full contact, while others have several revolutions of slack in the gears to compensate before they are pulling any of the load. This means that in worst case a single pinion is holding the entire load from the wind requiring very high safety factors throughout the design of the turbine.

When the yaw system is designed the design loads are based on simulations of the specific wind turbine in different wind conditions. These loads are extrapolated and are hence the foundation of the design. As the nature of the wind is stochastic, the system has to be designed for very random occurring situations. The fatigue loading of the yaw system is mainly due to the turbulence in the wind flow on the rotor plane and the so-called 3p loading on the system. The 3p loading is the load amplitude occurring three times per revolution of the rotor. The ultimate loading of the system could for example be the "50-year gust" or "100-year storm", which, as the names state, properly would not occur during the turbines life time. Designing a yaw system which is able to operate under these load conditions or

even hold the nacelle fixed would lead to very large and expensive systems, so what is normally done is to let the system slide during extreme loading. However, letting a friction based system slide may introduce very unwanted dynamic behavior, where the system might slide uncontrollable fast, tearing the yaw system apart.

Based on this knowledge, there is an increased interest in developing new systems to avoid these problems. A thorough state of the art analysis on hydraulic yaw systems have been conducted in Stubbier and Pedersen (2011b). None of the references present results from measurements or dynamic simulations of the concepts presented, why this paper focuses on dynamic results from modeling as well as test rig measurements in order to cover the question of how a hydraulic soft yaw system actually behaves under the dynamic loading of a wind turbine.

In order to introduce a hydraulic replacement of the electrical yaw system it is necessary to convince the wind turbine manufactures that the design will introduce the promised features along with documentation of the wind turbine and system behavior during loading.

The yaw system is designed based on loads extracted from the aero-elastic code FAST and the NREL 5 MW (Jonkman et al., 2009) standard wind turbine. Further a full hydraulic and mechanical model is derived and co-simulated with the full wind turbine model in order to be able to extract knowledge of which influence the yaw system might have on the wind turbine behavior.

The model of the hydraulic yaw system is validated up against a full scale workshop test rig, which is presented in this paper. The combination of the full scale workshop test rig and the model of the system are important in the process of getting this new technology proven for a wind turbine prototype.

Focus of this paper is hence on the design of the hydraulic yaw system and the experimental validation of the system, based on a hereto developed test rig, which may be used to emulate the wind turbine behavior and interaction with the yaw system. This paper first presents the system design of the hydraulic yaw system followed by a model description. The model is co-simulated with the full wind turbine code as a proof of concept, before measurements from the test rig are presented and the model is experimentally validated. Based on the results and discussion of these it is found that the hydraulic system shows the desired behavior and that the model resembles the system sufficiently well to be used for co-simulation and design purposes of wind turbine OEMs.

2 System Description

The test rig system is designed based on loadings extrapolated from the NREL 5 MW turbine (Jonkman et al., 2009) and standard IEC Design Load Cases (DLCs). Practical limitations with the number of motors it is possible to fit on a standard yaw bearing however required a downscaling of the test system, which means that the most extreme load cases may not be tested for. This will however be possible through simu-

lations, once the model is verified. The test rig is designed for maximum loading of approx. 3 MNm, where the load range for a 5 MW turbine will be in the order of 2 - 3 MNm for nominal load and 18 MNm for extreme load. The difference between nominal and extreme load is that the system must be able to withstand nominal load in normal operating conditions, whereas the extreme load is based on for example a 50 year wind gust and hence only happens once in a turbines lifetime.

The test rig is divided in two sub-systems, a hydraulic and an electrical. The system schematic is shown in Fig. 2. The electrical part of the system, consisting of 8 AC motors with individual servo control, is used to emulate the wind loads on the hydraulic system. The loads are transferred by the gears connected to the electrical motors, through the pinion to the tooth rim. The tooth rim is also connected to the pinion on the gears coupled to the hydraulic motors. The interaction between the loads and the movement of the yaw system is not trivial to emulate, since there is no inertia corresponding to the nacelle inertia in the system. It should therefore be noticed that the loads applied to the system by the electrical motors are simulated loads on the yaw system, from simulations where the hydraulic yaw system have been included. Hence the loads from simulations correspond to the loads the system should handle in reality, assuming similar behavior of the test as in the simulation model. However, when the system is yawing actively, the nacelle inertia is missing and there is a need for emulation of this inertia by the electrical motors. The loads from the inertia will however be accounted for in the co-simulations described in section 6.

The hydraulic yaw system considered in the following is designed to withstand the above load cases. For a more profound analysis of the requirements to the hydraulic yaw system and the development of the yaw system please see Stubkier and Pedersen (2011a) and Stubkier et al. (2011). The concept of the system is

shown in Fig. 2. The schematics of Fig. 2 includes; (1) Suction Filter, (2) Charge pump, (3) Pressure relief valve for flushing, (4) Pressure relief valve for charge system, (5) High performance gas loaded piston accumulators, (6) pressure relief valves, (7) Internal gear motor/pumps, (8) Flushing valve, (9) Check valves, (10) Pressure relief valve, (11) Logic element for over load protection, (12) 2/2 valve, (13) Pressure relief valve, (14) Swash plate pump, (15) Flow control valve, (16) Filter for swash plate pump, (17) Variable orifice.

The hydraulic yaw system presented in Fig. 2 has two operating modes; active and passive. In the active mode, the system is yawing, turning the rotor plane up into the wind or unwinding the cables which run through the tower. This mode is controlled by the 2/2 valves (12) which are opened, where after the flow to the system is controlled by the swash plate pump (14). An alternative configuration could be to use a unidirectional pump and a 4/3 valve instead, but this will be based on economic considerations for the components in question. In the active mode the pressure builds up simultaneously on the eight hydraulic motors due to the fact that they are connected in parallel. This means that regardless of backlash, the motors will all be loaded with the same torque, evening out the load on the pinions.

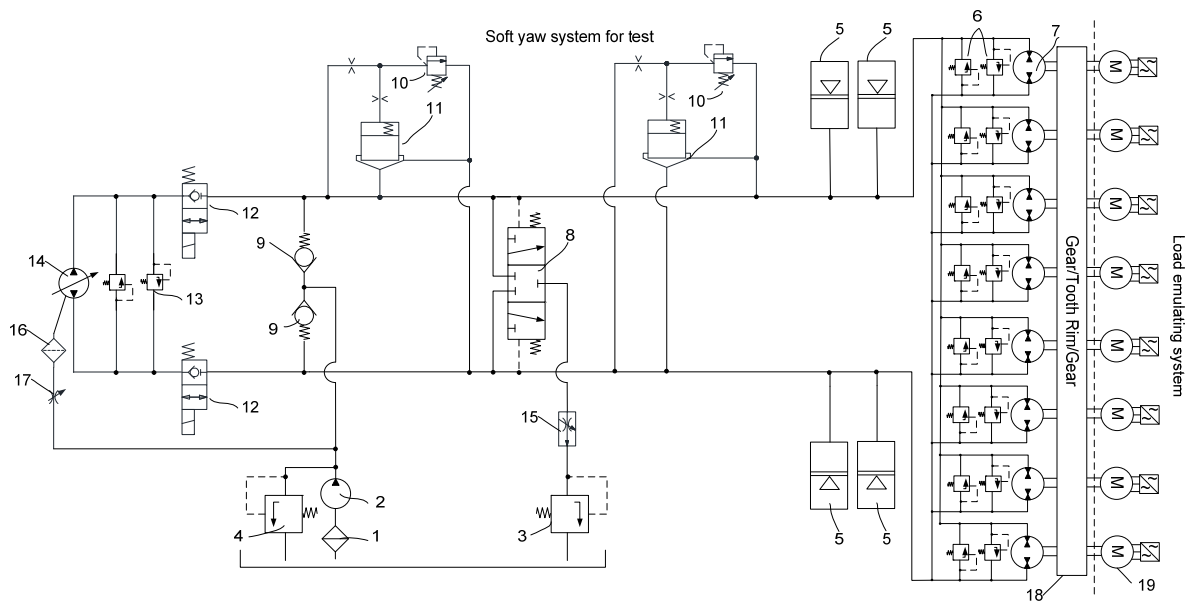


Fig. 2: System schematics of the full scale test rig

In passive mode the system is working as a soft yaw system, see Stubbier and Pedersen, 2011. Here the 2/2 valves are closed at all times and the swash plate pump turned off. When the system is loaded by a wind gust on the rotor plane, the eight hydraulic motors operate as pumps driving oil from one side to the other. The oil fills up the accumulator on the high pressure side and drains the accumulators on the low pressure sides. When this happens the pressure drop across the hydraulic pumps increase giving higher resistance to the wind loading. This can continue until the pressure reaches the predefined maximum pressure of the shock valves (6) or the hydraulic logic (10, 11). When either opens, flow is led from the high pressure side to the low pressure side letting the system yaw and hence avoiding extensive loading of the pinions in the yaw gearing.

3 System Dimensioning

A challenge in designing the hydraulic yaw system is finding appropriate components. The following section describes the dimensioning of the main components of the system shown in Fig. 2.

A picture of the full scale test rig is shown in Fig. 3. To give an impression of the dimensions of the setup the diameter of the motor-pump configuration is approx. 2.2 m.

3.1 Motor/Pump

The motors chosen for the hydraulic yaw system are of the internal gear type. The utilized motors are especially designed for four quadrant operation, meaning that they can operate as both motor and pump in both directions. The motor-pump units are designed for rough duty cycles with highly intermittent loads, i.e. many start, stop and direction changes, which normal hydraulic motors do not handle well.



Fig. 3: Picture of the full scale test rig

The motors have a displacement of 32.3 cc/rev and a maximum torque at 164 Nm each. Eight of these combined with the gear ratio of 1:4407.3 yields a maximum yaw torque of 5.8 MNm. The gear itself has a ratio of 323.7:1, while the pinion tooth-rim has a gear ratio of 177:13.

The nominal operating speed for the motors during yawing will therefore be 220 rpm, corresponding to yaw speed of 0.3°s^{-1} . The flow to the system during yawing at 0.3°s^{-1} is then 56 l/min.

The rotational speed of the motors is relatively low compared to nominal speed of the motors, but still within the reasonable range. A further improvement could be to raise the gear ratio. Another option would be to make the system yaw faster; the latter is, however, not in agreement with the IEC standard for yaw system design. Considering the duty cycles for the yaw motors, these will however operate at relatively low speed, even if raising the gear ratio, why testing the motors at this low speed is one of the most important test to be performed in the test rig. Hence for the first design the gear ratio is not altered.

The eight hydraulic motors are connected four-by-four in manifolds to ensure that the maximum flow seen in the individual manifolds is only the sum of four motors and not eight. This way the components utilized may be kept within standard series production components, reducing the cost of the system.

3.2 Accumulators

The accumulators on the test rig system consist of two times two 12.5 liter piston-type, gas-charged, hydraulic accumulators. These accumulators are widely used and thoroughly tested within the wind turbine industry. However, it might turn out to be beneficial to use bladder accumulators instead due to the many small duty cycles. Further analysis of the systems behavior is however required to determine this.

Assuming that the accumulators are half full when the system is in equilibrium, and have a minimum gas volume of 0.5 liter when full, the allowed deflection of the yaw system is 3.8 degrees:

$$\frac{12/360^{\circ}}{0.032/8.4407.3} = 3.8^{\circ} \quad (1)$$

The pre-charge pressure p_{pc} of the accumulators is set so that the pressure when the accumulator is half full corresponds to the boost pressure $p_{1/2}$ of the system at 20 bar. This way, the accumulators may be half filled with the boost pump, and will not be emptied more than half by the flushing system. According to the ideal gas behavior of the system, adjusted with the adiabatic constant $\kappa = 1.4$ the pre-charge pressure of the system is set to

$$p_{pc} = p_{1/2} \cdot \left(\frac{V_{1/2}}{V_{pc}} \right)^{1.4} = 7.5\text{bar} \quad (2)$$

The manifolds for the accumulators are designed such that the accumulators may be mounted directly on the manifolds without usage of any hoses, tubes or fittings allowing much higher peak flow.

3.3 Pressure Relief Valves

The cartridge pressure relief valves (6) are for the test rig purpose set to a cracking pressure of 145 bar and a maximum flow of 70 l/min. The logic components (11) have a nominal flow of 850 l/min, which corresponds to a shaft speed of approx. 3300 rpm on the hydraulic motors.

3.4 Cooling and Flushing

Cooling of the system is an issue since the loads from the wind must be turned into heat. The system is based on a closed circuit, so a flushing system including a flushing valve and a boost pump is implemented. This is, however, not a straight forward task since both of the sides are connected to hydraulic accumulators. When the flushing valve (8) opens due to a pressure difference, the accumulators in the side with the lowest pressure will be drained until the pressure stabilizes at the pressure setting of the pressure relief valve between the flushing valve and tank (3) on Fig. 2. The cracking pressure of this valve is normally set relatively low in order to avoid draining the system from high pressure in the low pressure line. The boost pump must be able to deliver the power corresponding to the pressure setting of the relief valve and the flow setting of the flow control valve (15). Hence increasing the crack pressure of the pressure relief valve yields a higher power usage from the boost pump.

The flushing system is designed with a flow control valve, which is set to 30 liters per minute. This in the combination with the accumulator pre-charge pressure yields that the boost pump must be able to deliver 30 liters per minute at 20 bars to keep the system from draining. In addition the internal and external leakage in the system must be added to the boost pump requirement. The flushing system needs a pressure drop of 7 bars to open.

3.5 Pump Station / PowerPack

The pump station for the hydraulic yaw test rig is based on a 22 kW AC motor driving a 100 cc variable axial piston pump (14). This setup is used for the test setup for ease of control and simplicity. The setup of the pump and power pack in the final system for implementation in wind turbines are bound to look different due to cost and control demands.

The boost pump is designed with a 3 kW AC motor driving a 22 cc gear pump at 1440 rpm ideally yielding 31.7 l/min at 54 bar. Due to the efficiency of the boost pump the effective pressure and flow limits are lowered.

3.6 Electrical load System

The loading on the system, shown in Fig. 2, which emulates the wind forces on the yaw system, is generated by eight electrical 2.2 kW AC servo units. These motors are also connected to the yaw tooth rim by the same type of gear as the hydraulic motors. However, the gears have one stage more yielding a combined gear ratio of 1:14080.

The motors each have a maximum torque of 27 Nm and a bandwidth for torque well above the 2 Hz 3p load on the turbine yaw system. The maximum combined torque from the electrical drives with gears is hence 3 MNm, which is approximately the maximum load the yaw system will have to deal with under normal operating conditions. Higher extreme loads might occur, but may only be partly emulated by the test bench.

3.7 Gears

The gears are of the normal industrial planet gear type and normally have a gear ratio of 1:1034.1. The same gears are used for the electrical drives as for the hydraulic motor/pump units. For the hydraulic side, the gear ratio is however lowered with a factor of ~3.2 by removal of the first gear step, resulting in a gear ratio of 1:323.7.

There will be gear slack and stiffness issues in the gears due to the relatively cheap gear with a high gear ratio and four stages. The slack in the gears is three revolutions on the input shaft for the electrical drives and one revolution for the hydraulic drives, due to the high gearing ratios.

4 System Model

The equations describing the dynamic behavior of the yaw system are presented in the following. Based on the developed model simulation results of the system are presented in the next section and compared to measurements from the test rig. The schematics of the model are shown in Fig. 2.

4.1 Nacelle Inertia Dynamics

The nacelle dynamics is described by the following equations

$$I \ddot{\theta} = \begin{cases} (M - C \cdot \text{sign}(\dot{\theta}) - B \cdot \dot{\theta}) & |M| > C \wedge \dot{\theta} \neq 0 \\ 0 & |M| < C \vee \dot{\theta} = 0 \end{cases} \quad (3)$$

$$M = M_{\text{yaw,load}} - M_{\text{yaw,sys}} \quad (4)$$

where C is the coulomb friction coefficient, B is the viscous friction. M is the resulting torque from aerodynamic loading and the torque from the hydraulic yaw system. I is the inertia of the nacelle, which in this case is represented by the inertia of the tooth-rim and hydraulic- and electrical motors and gears. Further, the loading applied to the yaw system includes the dynamics of the inertia, since it is extrapolated from simulations including the inertia.

4.2 Hydraulic Yaw System Dynamics

With the displacement of the hydraulic motors, D , described in SI units m^3/rad the torque from the hydraulic motors can be described as

$$M_{\text{yaw,sys}} = k_m \cdot \Delta p \cdot D \quad (5)$$

Where $k_m = n_{\text{hyd, motor}} r_{\text{gear}}$, m , is the number of hydraulic motors multiplied with the total gear ratio of the yaw system. The expression does not take into account the hydro-mechanical efficiency of the motor, as friction is accounted for separately.

The flow through each hydraulic motor is described as.

$$Q_{\text{nom}} = D \cdot \dot{\theta} \cdot \eta_{\text{vol}} \quad (6)$$

where Q_{nom} is the nominal flow and η_{vol} is the volumetric efficiency depicted in Fig. 4

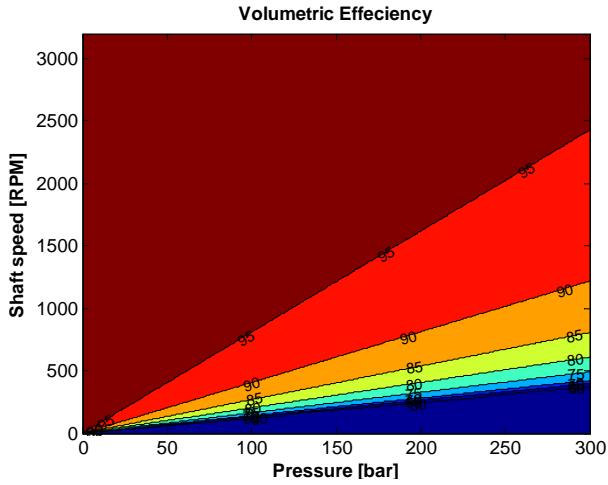


Fig. 4: Volumetric efficiency for hydraulic motor/pump units. Values based on pump manufacturer data. Corner operation below 500 rpm and 50 bar made based on extrapolated data

4.3 Accumulator Dynamics

Based on the research by (Otis and Pourmovahed, 1985) the following equations can be utilized for the gas loaded accumulators.

The energy equation for the system for the accumulator is defined as

$$m\dot{u} = \dot{Q} - \dot{W} \quad (7)$$

where m is the mass of the gas and u is the specific internal energy of the gas. \dot{Q} is the heat transfer and \dot{W} is the work done by the accumulator piston. \dot{Q} is described by

$$\dot{Q} = m \cdot c_v \cdot \frac{(T_s - T)}{\tau} \quad (8)$$

where c_v is the specific heat, T_s the ambient temperature and T the gas temperature. The thermal time constant describes the rate of the heat dissipation between the inside of the accumulator walls and the gas. Experimental identification of this value requires dynamic gas temperature measurements and even fast thermocouples have too large time constants to measure this dynamic behavior accurately. Laser and inferred sensors all measure the surface temperature of the accumulators, why this also would give misleading values. The time constant is therefore based on experience where $\tau = 8$ s is found appropriate for the accumulators utilized in this system.

The rate of piston work is defined as

$$\dot{W} = p \cdot \dot{V} \quad (9)$$

where p is the gas pressure and V is the volume of the gas. When

$$du = c_v \cdot dT + \left(T \cdot \left(\frac{\partial p}{\partial T} \right)_v - p \right) dv \quad (10)$$

and v is the specific volume of the gas, the energy equation is derived as

$$\dot{T} = \frac{T_s - T}{\tau} - \frac{T}{c_v} \cdot \left(\frac{\partial p}{\partial T} \right)_v \cdot \dot{v} \quad (11)$$

The well-known Benedict-Webb-Rubin equation defines the p - v - T relationship

$$p = \frac{R \cdot T}{v} + \frac{B_0 \cdot R \cdot T - A_0 - \frac{C_0}{T^2}}{v^2} + \frac{b \cdot R \cdot T - a}{v^3} + \frac{a \cdot \alpha}{v^6} + \frac{c \cdot \left(1 + \frac{\gamma}{v^2} \right) \cdot e^{-\frac{\gamma}{v^2}}}{v^3 \cdot T^2} \quad (12)$$

where R is ideal gas constant. The eight other constants are outlined in Table 1.

Table 1: Constants in the Benedict-Webb-Rubin equation

Constant Name	Value
a	0.025102
A_0	1.053642
b	0.0023277
B_0	0.0407426
c	728.41
C_0	8059.00
α	0.0001272
γ	0.005300

Differentiation of Eq. 12 and substituting it into equation Eq. 11 yields

$$\dot{T} = \frac{T_s - T}{\tau} - \frac{\dot{v}}{c_v} \cdot \left[\frac{R \cdot T}{v} \cdot \left(1 + \frac{b}{v^2} \right) + \frac{1}{v^2} \cdot \left(B_0 \cdot R \cdot T + \frac{2 \cdot C_0}{T^2} \right) - \frac{2 \cdot c}{v^3 \cdot T^2} \cdot \left(1 + \frac{\gamma}{v^2} \right) \cdot e^{-\frac{\gamma}{v^2}} \right] \quad (13)$$

By this equation the temperature change in the hydraulic accumulator is defined by a change of volume in the accumulator gas. However, the specific heat of the gas changes with pressure based on the thermodynamic definition:

$$\left(\frac{\partial c_v}{\partial v} \right)_T = T \cdot \left(\frac{\partial^2 p}{\partial T^2} \right)_v \quad (14)$$

Based on well-known values of the specific heat at low pressure, the specific heat can be found by the following expression:

$$c_v = c_v^0 + \int_{-\infty}^0 T \cdot \left(\frac{\partial^2 p}{\partial T^2} \right)_v dv \quad (15)$$

By utilization of the Benedict-Webb-Rubin in Eq. 14 the specific heat may be expressed as:

$$c_v = c_v^0 + \frac{6}{T^3} \cdot \left(\frac{C_0}{v} - \frac{c}{\gamma} \right) + \frac{3 \cdot c}{T^3} \cdot \left(\frac{2}{\gamma} + \frac{1}{v^2} \right) \cdot e^{-\frac{\gamma}{v^2}} \quad (16)$$

The value of c_v^0 can be approximated by:

$$c_v^0 = R \cdot \left(\frac{N_1}{T^3} + \frac{N_2}{T^2} + \frac{N_3}{T} + (N_4 - 1) + N_5 \cdot T + N_6 \cdot T^2 + N_7 \cdot T^3 + N_8 \cdot \frac{N_9^2}{T^2} \cdot e^{\frac{N_9}{T}} \cdot \left(e^{\frac{N_9}{T}} - 1 \right)^{-2} \right) \quad (17)$$

For the values of N_i found in Table 2.

Table 2: Constants for the ideal gas specific heat for nitrogen

Constant Name	Value
N_1	735.210
N_2	34.224
N_3	-0.557648
N_4	3.5040
N_5	-1.7339E-5
N_6	1.7465E-8
N_7	-3.5689E-12
N_8	1.0054
N_9	3353.4061

By combination of the above equations, the pressure of the nitrogen gas may be calculated based on temperature and specific volume and hence a force/pressure equilibrium between the gas and oil. The dynamic behavior of the accumulator piston is not included in the model, as the states of the piston are of no interest. The uncertainty added to the model by this simplification is the pressure difference between the gas and oil side arising from the friction in the accumulator piston. Considering that the sealing and guide rings are specially designed in teflon and PTFE for low friction and smooth running even at low speeds, the friction in the accumulators is very low – also compared to the friction in the rest of the system (gears, bearing etc.). It may therefore be neglected in the modeling, without introducing much of an error.

4.4 Control Valves Dynamics

The valves are modeled by the orifice equation as:

$$Q = A(x_v) \cdot C_d \sqrt{\frac{2}{\rho} |\Delta p|} \cdot \text{sign}(\Delta p) \quad (18)$$

Which is valid for sharp edged orifices when also assuming turbulent flow. To account for low Reynolds numbers the discharge coefficient is evaluated as (McCloy and Martin, 1980)

$$C_d = C_{d,\max} \cdot \tanh\left(\frac{2\lambda}{\lambda_{\text{crit}}}\right) \quad (19)$$

where λ is the Reynolds flow number and λ_{crit} is the critical flow number for the first iterations set to 1000.

The dynamics of the valves is simply described as a second order system with a natural frequency and a damping ratio.

Since the valve dynamics is defined as natural frequency and damping ratio the valve can be described as:

$$\begin{bmatrix} \dot{x} \\ \ddot{x} \end{bmatrix} = \begin{bmatrix} 0 & 1 \\ -\omega_n^2 & -2\zeta\omega_n \end{bmatrix} \begin{bmatrix} x \\ \dot{x} \end{bmatrix} + \begin{bmatrix} 0 \\ \omega_n^2 \end{bmatrix} k \cdot u \quad (20)$$

where ω_n is the valve eigenfrequency, ζ the damping, k is the gain between input signal and spool position and u is the input signal.

4.5 Hose Dynamics

The pressure build up in the hydraulic hoses are described as a simple pressure build up in a hydraulic volume

$$\dot{p} = \frac{\beta_{\text{eff}}(q_{\text{in}} - q_{\text{out}})}{V_{\text{hose}}} \quad (21)$$

Where β_{eff} takes the air content and the expansion of the line walls into account.

$$\beta_{\text{eff}} = \frac{1}{\frac{1}{\beta_{\text{fluid}}} + \frac{1}{\beta_{\text{hose}}}} \quad (22)$$

Where β_{fluid} is the bulk modulus for the oils and β_{hose} is the bulk modulus for the hose material.

$$\beta_{\text{fluid}} = \rho_{\text{fluid}} \cdot \frac{dP}{d\rho_{\text{fluid}}} \quad (23)$$

Where ρ_{fluid} is the density of the hydraulic oil depending on temperature and pressure. The hose bulk modulus is described as

$$\beta_{\text{hose}} = \frac{1 + w_{\text{comp}} \cdot (P - P_0)}{w_{\text{comp}}} \quad (24)$$

Where

$$w_{\text{comp}} = \frac{2}{E} \left(v + \frac{r_o^2 + r_i^2}{r_o^2 - r_i^2} \right) - \frac{2}{E} \cdot v \cdot \frac{r_i^2}{r_o^2 - r_i^2} \quad (25)$$

where E is Young's modulus, v is Poisson's module and r_i and r_o is the inner and outer radius respectively.

4.6 Pressure Relief Valves

The pressure relief valves are simply described by

$$Q = \begin{cases} \Delta p \cdot k_{\text{qp}} & \Delta p > 0 \\ 0 & \Delta p < 0 \end{cases} \quad (26)$$

where

$$\Delta p = p_{\text{in}} - p_{\text{out}} - P_{\text{crack}} \quad (27)$$

and k_{qp} is the flow pressure coefficient for the given pressure relief valve. P_{crack} is included in the equation to avoid flow through the valve when $p_{\text{in}} - p_{\text{out}}$ is below the cracking pressure of the pressure relief valve.

4.7 Check Valves

The flow through the check valves are described by the before mentioned orifice equation. The opening area of the check valve is linear dependent on the valve position which is described as

$$x = \begin{cases} 0 & \Delta p < P_{\text{crack}} \\ \frac{\Delta p - P_{\text{crack}}}{k_{\text{spring}}} & P_{\text{crack}} < \Delta p < P_{\text{stop}} \\ x_{\text{max}} & \Delta p > P_{\text{stop}} \end{cases} \quad (28)$$

where P_{crack} is the cracking pressure, k_{spring} is the stiffness of the check valve and P_{stop} is the pressure for full opening.

4.8 Electrical Motors

The electrical motors are considered as perfect torque control actuators due to the bandwidth of the servo drives controlling them, why they are simply modeled as inertias with friction and damping.

4.9 Reduction Gears

The reduction gears are modeled as inertias connected with a spring and damper system. As the models including backlash are simply too heavy computational wise, when including 16 gears with individual backlash or even worse 16 gears each with four stages of backlash, then the backlash is modeled as included in the stiffness of the system, i.e. as a part of the spring effect. This way of modeling the gears are of course a rough estimation, but as shown late it will do for the purpose of this model.

5 Model Verification

This verification is based on the ‘passive’ case, when the yaw system is deflecting due to turbulent loading on the rotor plane.

When considering the model for verification the following states are of particular interest; Accumulator pressure, Hydraulic motor torque, Hydraulic motor speed and Electrical motor speed, which are all considered in order to verify that the model is acting as suspected. Figure 5 shows the load applied to the test rig in the verification experiment. The loads applied are taken from a load case of average wind speeds of 12 m/s, no yaw error and normal turbulence – which is the IEC DLC 1.2 @1 2 ms NTM load case. This load is applied by the eight electrical servo drives. The load amplitude and frequency are based on the NREL 5 MW turbine downscaled to fit the test rig. The dominating frequency is, as before mentioned, the so called 3p frequency, which is three times the rotor rotation frequency, which corresponds to the frequency by which a blade passes the tower.

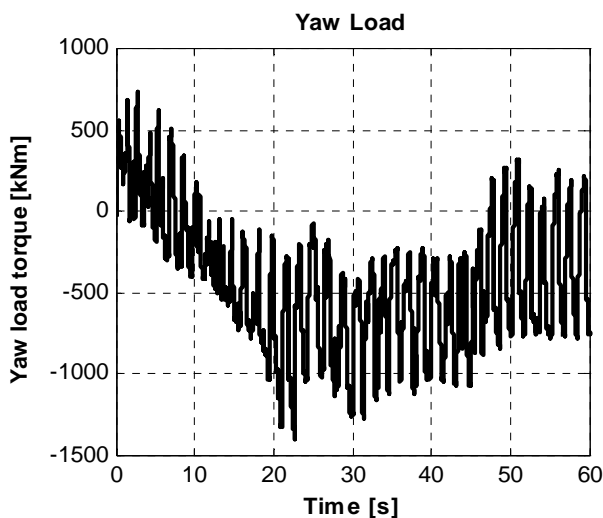


Fig. 5: Yaw loads applied to test rig

The absolute speed of the hydraulic motor/pump units is shown in Fig. 6, where the simulation model is

compared to the measurements. There is some difference between the simulated and measured results, but the overall picture shows the right tendencies in frequency and amplitude. The differences between the results are due to the simplification of the gears, which related to both those coupled to the electrical side and the hydraulic side.

The results presented in Fig. 5 and Fig. 6 are for a real load case, where slack in the gears is significant for the results. For this reason Fig. 7 shows the response of the hydraulic motors to a slower more well defined torque ramp input as shown in Fig. 8. From this it may be seen that overall the simulated response shows good resemblance with the measured. There is, however, a difference in peak velocity at 4s. The difference has it root cause in the modeling of the gear units, which as mentioned are modeled as simple inertias in connection with a spring and damping unit.

When the system is to be used for the co-simulation interface described in section 7, this error will, however, be more than halved, since the electrical load system no longer is included, hereby removing the error resulting the electrical side.

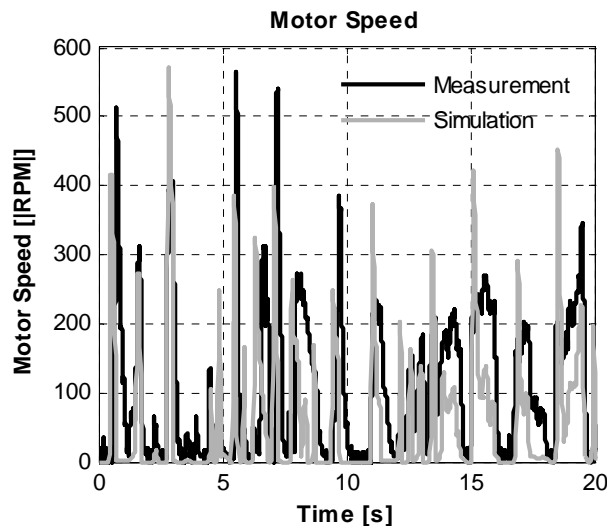


Fig. 6: Measured and simulated motor speed during DLC 1.2

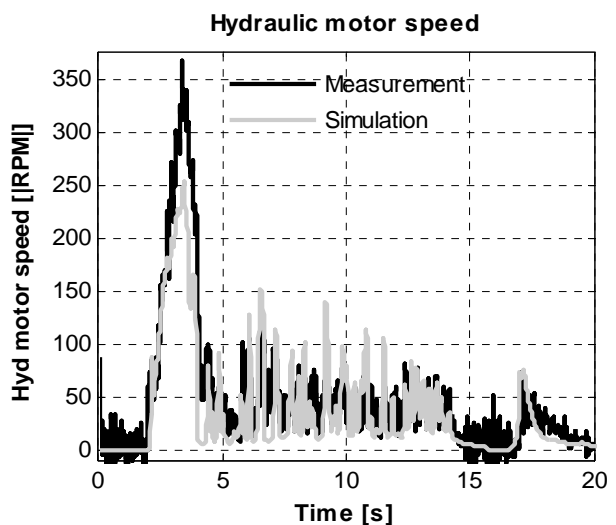


Fig. 7: Hydraulic motor speeds, when the system is applied a slow torque ramp

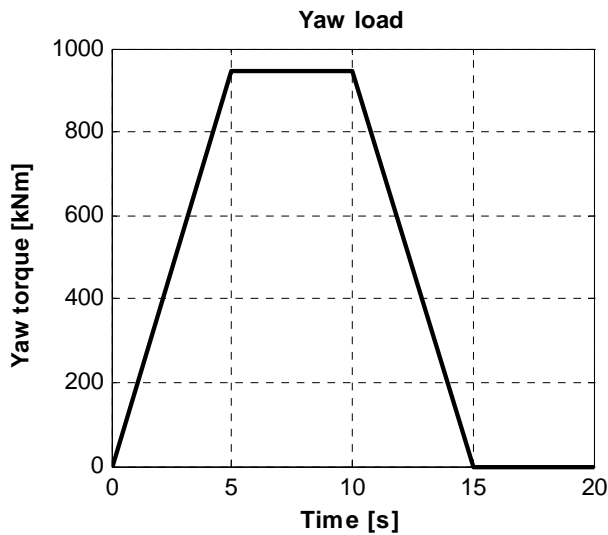


Fig. 8: Slow torque ramp for motor speed verification

However, if Fig. 9 is considered, where the torque on a hydraulic motor is shown, there is a very good agreement between simulated and measured results. The hydraulic motor torque is depending on various states in the system, such as friction, accumulator dynamics, volumetric efficiency of the hydraulic motors and stiffness of the gears. This makes the torque on the hydraulic motor shafts a very good indicator of system resemblance. The loading of the hydraulic motors is furthermore the single most important state for feedback to the FAST co-simulation interface as illustrated in Fig. 15.

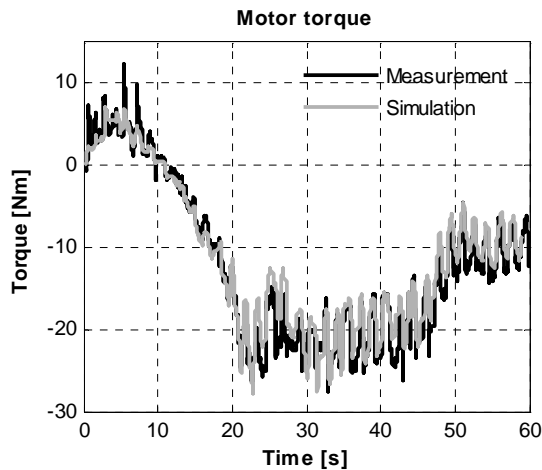


Fig. 9: Measured and simulated hydraulic motor torque during DLC 1.2

The accumulator pressures shown in Fig. 10 also confirm that the hydraulic model gives a good idea of the behavior of the test rig system. There are some differences due to the complexity of external and internal leakage in the system in combination with the charge pump system, but the overall system performance, pressure levels and frequencies are well captured in the model.

The yaw angle is shown on Fig. 11. It should be noticed that the movement is based on the position of the electrical motors, since it is currently not possible to measure the yaw angle directly. This means that the

dynamics of the gear is included in this measurement. Otherwise it shows that the movements are relatively small as expected.

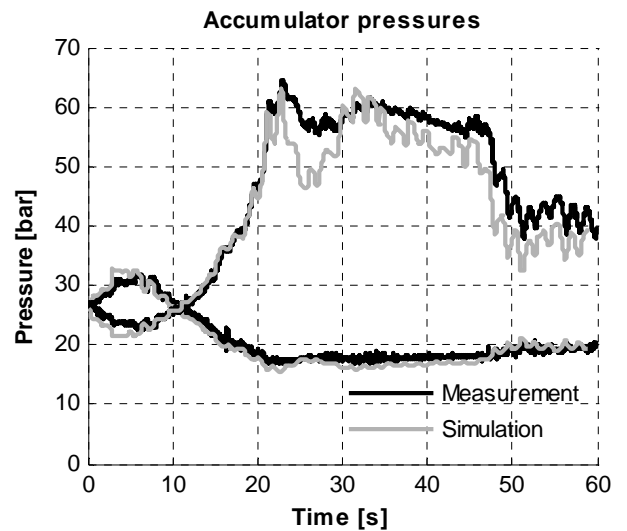


Fig. 10: Measured and simulated accumulator pressures during DLC 1.2 12 m/s NTM

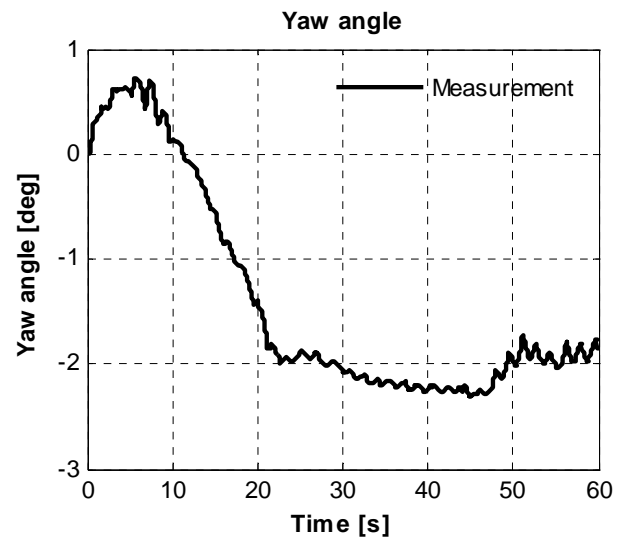


Fig. 11: Measured yaw angle during DLC 1.2

Based on the above results and similar results for other DLC's the model is therefore found to represent the real systems sufficiently well for further analysis and design purposes, in combination with the aerodynamic code.

6 Different DLC Measurements

In order to test the system properly different design load cases may be applied. The loadings are extrapolated from FAST and afterwards applied to the test rig.

The loading of the test rig is shown in Fig. 12, where it may be seen that the loading rises significantly with the wind speed. The pressures on the A and B side of the hydraulic motors are shown in Fig. 13 for the three different design load cases; 7 m/s, 12 m/s and 18 m/s and using the normal turbulence mode. It is actually possible to extract a lot of rough information

on the yaw system behavior from the pressure curves, including loading, yaw angle and yaw speed. However, the dynamic behavior of the accumulators described in the above indicates that the pressure in the accumulator is depending on the speed with which the accumulator is filled or emptied. This is evident from Fig. 14, where the yaw angle during the different loading cases is shown. Interestingly, the maximum absolute yaw angle for the 12 m/s and the 18 m/s load case is approx. the same. After 30 seconds the 12 m/s yaw angle actually exceeds that of the 18 m/s load case even though the loading at that point is 50 percent higher. This is due to the increase in gas temperature in the 18 m/s load case which is much higher than for the 12 m/s load case.

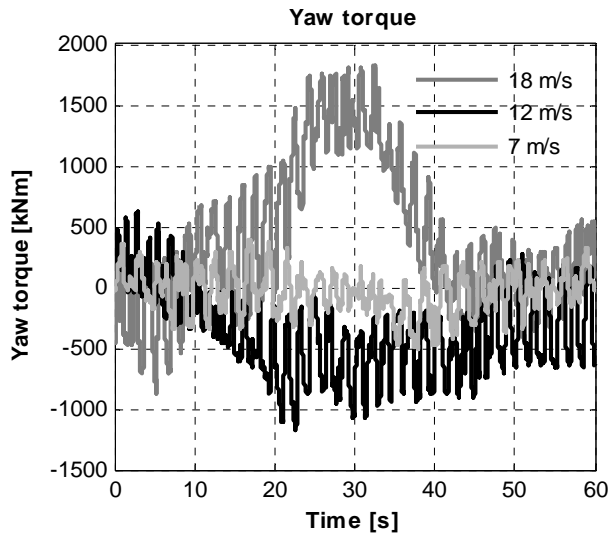


Fig. 15: Yaw loads applied during different DLC's

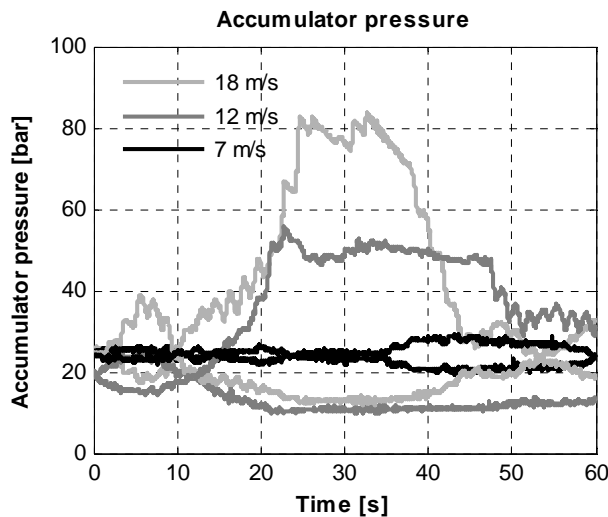


Fig. 13: Accumulator pressures under different DLC's and normal turbulence

These results clearly show that the soft yaw system is progressive since the harder the system is loaded, the stiffer it gets. This is a very desirable feature, since it ensures that the system never deflects too much compared to the original wind direction. This is desirable as the turbine should not sway too much compared to the set reference angle in order not to lose too much power production capability or to impose large loads on the

turbine structure due to loads from the inertia acceleration.

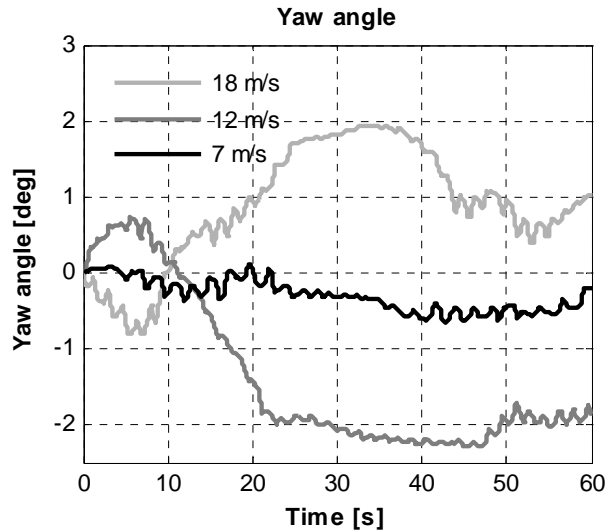


Fig. 14: Yaw angle under different DLC's

Internal leakage in the motors will of course mean that the motors may creep over time. This is however not considered a problem, as the yaw control system will ensure that the system is actively yawed back in position. Compared to the movements of the yaw system, the leakage in the motors is however limited, why not considered a problem as the soft yaw system not is supposed to be kept in one position over a long period of time.

7 Co-Simulation with FAST

Based on the above verified model of the system, a co-simulation between the hydraulic system and the complete FAST model may be set up to analyze the correct feedback from the yaw system when interacting with the rest of the turbine, which may also be used for future tests of closed loop control of the yaw angle. The 5 MW NREL turbine in FAST is setup to exchange information with the model of the test rig such that they interact dynamically with each other as illustrated in Fig. 15. This way the aero-dynamic feedback from the turbine blades may be taken into account along with the changing inertia due to the rotation of the blades on the turbine. When the hydraulic model feeds back the yaw torque to the full turbine code, the yaw torque is included in the dynamics for the turbine, hereby integrating to a new yaw speed, which is sent to the hydraulic model of the yaw system. Connecting the verified hydraulic model with the verified FAST model gives a very good picture of the turbine behavior when utilizing the hydraulic soft yaw system.

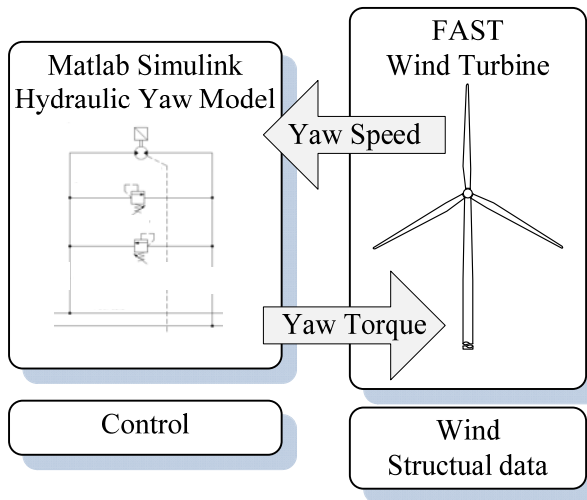


Fig. 9: Co-Simulation interface

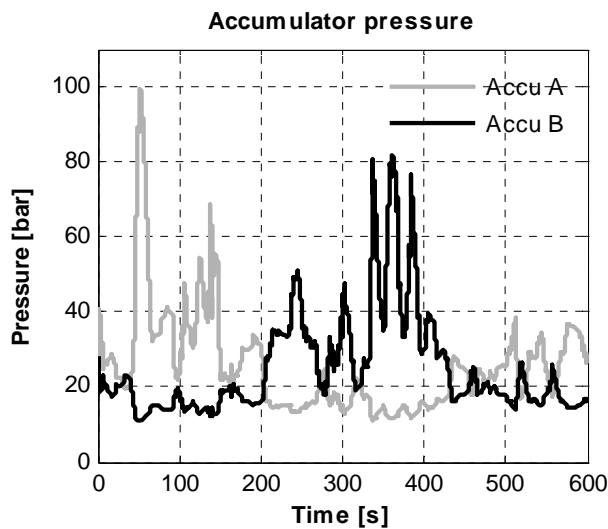


Fig. 10: Accumulator pressures during the DLC 1.2 12 m/s NTM load case

As shown in Fig. 10 the accumulator pressures keep well within reasonable range during this design load case.

The movement of the yaw system is shown in Fig. 17, where it may be seen that the system deflects up to approx. 3 degrees at 50 s and at 150 s. Considering the pressures in the accumulators at these two points it is obvious that the pressure difference is higher at 50 s than at 150 s although the deflection is the same. This is due to the dynamics of the gas in the accumulators, which depends on both pressure, volume and temperature. Hence if the gas temperature, which is shown in Fig. 12, is high the system becomes stiffer. This is a very nice property of the gas filled accumulators since it makes the “suspension system” progressive, making it more stiff if there is high turbulence, limiting the movements of the system. Considering the gas temperatures it is also evident that the temperatures are not too high to damage the sealing in the accumulators. The gas temperatures are high for shorter periods of time, but the average temperature is well below the nominal temperature for accumulator sealing.

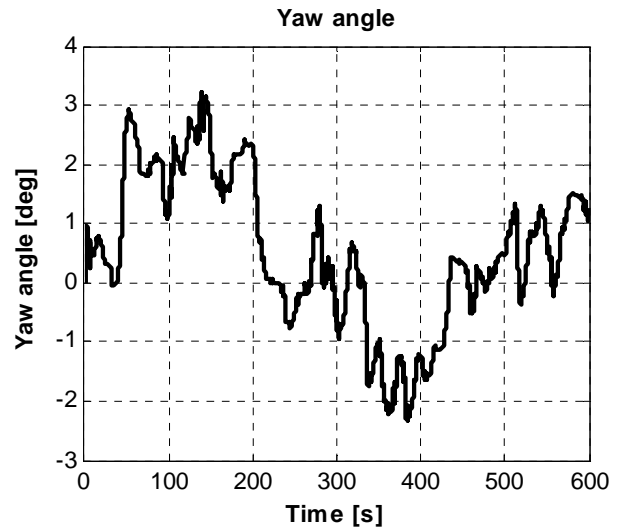


Fig. 11: Yaw angle during 12 m/s and normal turbulence

These results include the full dynamic behavior of the wind turbine including; blade deflection, nacelle inertia and feedback from the change in the lift and drag coefficients of the blades when the yaw angle is changed. Therefore this co-simulation setup is to be used for duty cycle analysis and test design for the different components throughout the yaw system.

The simulation setup is also used for the development of different control strategies for the yaw system, which would not be possible if the verified model had not been developed. The next step in the research therefore includes investigating the control possibilities for the soft hydraulic yaw system, which is not a trivial task, due to the accumulators in both pressure lines, which results in a very soft system. The new measures taken to this design is presented in Stubkier and Pedersen, 201x.

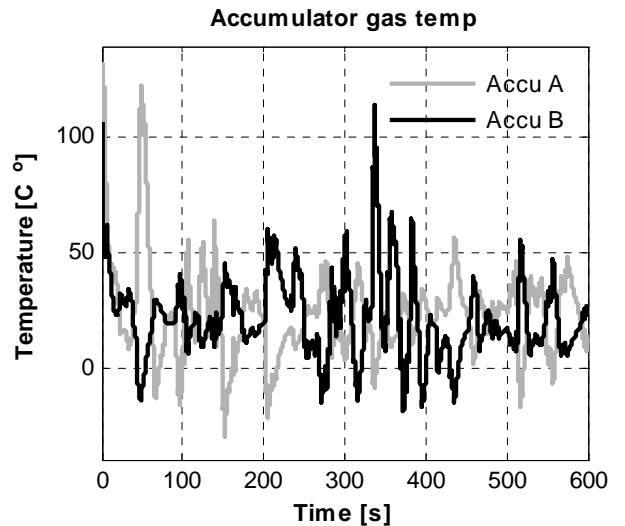


Fig. 12: Accumulator gas temperature during 12 m/s and normal turbulence

8 Conclusion

The paper presented a full scale test rig of a hydraulic yaw system for a multi MW turbine along with a mathematical model of the system in question. Simulation

results were presented and validated against measurements from the full scale test rig. These results are important in the process of getting the new technology accepted by the wind turbine manufactures. This could for example be done by testing of the simulation model in co-simulation with their wind turbine simulation code.

Further results from the test rig were presented, from loadings corresponding to a load case in 7 m/s and 18 m/s wind conditions. The results are to be used for designing stress test of the hydraulic motors in order to prove hardware compliancy to the demands from the wind turbine manufacture.

The results presented show that the system behaves as expected when implemented in a wind turbine, why the next step will include designed controllers for the yaw system and hopefully implementing the yaw system in a real turbine.

Nomenclature

p_{pc}	Accumulator pre-charge pressure	[Pa]
$p_{1/2}$	Accumulator pressure at half full	[Pa]
η_{vol}	Volumetric efficiency	[%]
τ	Thermal time constant	[s]
λ	Reynold's flow number	[-]
ν	Poisson's module	[Pa]
k_{qp}	Flow pressure coefficient	[m ³ /Pa]
P_{crack}	Cracking pressure	[Pa]
k_{spring}	Spring stiffness	[N/m]
$V_{1/2}$	Gas volume at half full	[m ³]
V_{pc}	Gas volume at pre-charge pressure	[Pa]
$A(x_v)$	Area depending on position	[m ²]
B	Viscous damping	[Nm/rad/s]
C	Coulomb friction coefficient	[Nm]
C_d	Flow coefficient	[-]
c_v	Specific energy	[J/kg]
D	Hydraulic displacement	[m ³ /rad]
E	Young's modulus	[Pa]
I	Nacelle inertia	[kg m ²]
m	Mass of gas	[kg]
p	Pressure	[Pa]
Q	Flow	[m ³ /s]
q_{nom}	Nominal flow	[m ³ /s]
R	Ideal gas constant	[J/mol K]
T	Gas temperature	[K]
T_s	Ambient temperature	[K]
u	Specific internal energy of gas	[J/kg]
v	Specific volume	[m ³ /kg]
β	Bulk modulus	[Pa]
θ	Nacelle yaw angle	[rad]
ρ	Density	[kg/m ³]

References

Jonkman, J., Butterfield S. and Scott, G., 2009. Definition of a 5-MW Reference Wind Turbine for Off-shore System Development, NREL

McCloy, D. and Martin, H. 1980. Control of Fluid Power: *Analysis and design, 2nd edition. Ellis Horwood Limited*

Otis, D. R. and Pourmovahed, A. 1985. An Algorithm for Computing Non flow Gas Processes in Gas Springs and Hydro pneumatic Accumulators, *Journal of Dynamic Systems, Measurement, and Control*, 107, pp. 93 - 95

Pedersen, F. T., Gottschall, J., Kristoffersen, Runge, J. and Dahlberg, J.-Å. 2011. Yawing and performance of an offshore wind farm, Proceedings, EWEA

(a) **Stubkier, S. and Pedersen, H. C.** 2011. Design, Optimization and Analysis of Hydraulic Soft Yaw System for 5 MW Wind Turbine Wind Engineering Vol. 35, pp 529 - 550.

(b) **Stubkier, S. and Pedersen, H. C.** 2011. State of the art-hydraulic yaw systems for wind turbines, *Proceedings of the 12th Scandinavian International Conference on Fluid Power, Tampere University of Technology, Finland*

Stubkier, S. and Pedersen, H. C. 201x. Investigation of Self -Yaw and its Potential using a Hydraulic Soft Yaw System for 5 MW Wind Turbine, submitted to Wind Engineering

Stubkier, S., Pedersen, H. C., Andersen, T. O. and Markussen, K. 2011. Preliminary findings of soft yaw concept, *Fluid Power and Mechatronics (FPM), 2011 International Conference on*, pp. 456 - 461.



Søren Stubkier, M.Sc.

Since 2008 a Master of Science in Electro Mechanical System Design from the Institute of Energy Technology at Aalborg University. Since 2010 employed at Hydratech Industries as R&D Engineer and industrial researcher (Ph.D fellow) in close corporation with Aalborg University. His research focuses on soft hydraulic yaw system solutions for multi-MW wind turbines and hydraulic subsystems for wind turbines in general.



Henrik C. Pedersen, PhD, M.Sc.

Since 2009 Associate Professor at Department of Energy Technology at Aalborg University in Denmark. Prior to that Assistant professor and PhD-student also at Aalborg University. Author of more than 50 papers. Research areas include analysis, design, optimization and control of mechatronic systems and components, with special focus on fluid power for wind and wave energy applications.



Torben O. Andersen, PhD, M.Sc.

Since 2005 Professor in Fluid Power and Mechatronic Systems at Institute of Energy Technology, Aalborg University, DK. Prior to that Associate professor at AAU and R&D engineer at Danfoss. Research areas include control theory, energy usage and optimization of mechatronic components and systems, mechatronic system design in general, design and control of robotic systems, modeling and simulation of dynamical systems.